Influence of air annealing on the structural, morphology and optical properties of ZnSe thin films by CW-CO$_2$ laser evaporation

Wuttichai Phae-ngam[1]*, Suebtarkul Suchat[1], Taswal Kumpeerapun[2] and Voravit Kosalathip[2]

[1]*Physics Program, Phranakhon Rajabhat University (PNRU), Bangkok, Thailand*
[2]*Department of Physics, King Mongkut's University of Technology Thonburi (KMUTT), Bangkok, Thailand*

*Corresponding author. Tel: (+66) 814662378; E-mail: p_mon_phy@hotmail.com

ABSTRACT

CW-CO$_2$ laser evaporation was used to deposit ZnSe thin films onto glass microscope slides. The films prepared were annealed in air at annealing temperatures of 100, 200 and 300°C. The effect of annealing temperature on the surface morphology, crystal structure and optical properties was investigated. All samples were seen to have an homogeneous surface morphology. The as-deposited and low temperature annealed ZnSe films exhibited the cubic phase. As the annealing temperature increased, a hexagonal phase developed and at 300°C the ZnO phase began to appear. The average crystallite size of ZnSe films increased from 23.84 to 49.64 nm on annealing at 200°C. Dislocation density, strain in the film and film thickness decreased when the annealing temperature increased up to 200°C. The optical band-gap of the as-deposited film was 2.76 eV decreasing to about 2.70 eV at the 200°C anneal. The introduction of the ZnO phase at 300°C decreased crystallite size whereas it increased film strain. This work shows an easy and economical way to control band gap, crystallite size and film strain in ZnSe thin films by annealing in air. The lack of a pre-heated substrate and the ability to control band gap energy by annealing provides a versatile alternative source of ZnSe film deposition for potential optoelectronic applications. Copyright © 2014 VBRI press.

Keywords: ZnSe; thin film; laser evaporation; CO$_2$ laser; air annealing.

Wuttichai Phae-ngam is a PhD, teaching staff in the Physics Program, Faculty of Science and Technology, Phranakhon Rajabhat University, Thailand. He is working on the thin film preparation of semiconductor and the application of high power laser.

Introduction

The semiconductor is an essential material in electronic device fabrication such as diodes, laser diodes (LD), light emission diodes (LED), sensors, solar cells, thermoelectric devices, etc. [1-6]. The band-gap energy is a very important property of the semiconductor and depends greatly on the material, for example, GaAs, ZnO, and ZnS having band-gap energies at 1.4 eV, 3.2 eV, and 3.6 eV, respectively [7-9]. The band-gap energy value is explained by the energy level of the atom through quantum theory [10-11]. ZnSe is a semiconductor material which has 2.70 eV band-gap energy (bulk band-gap) [12]. ZnSe has been applied to many devices such as hybrid solar cell [13], green-blue LED [14], laser source [15], etc.

ZnSe films can be prepared by chemical vapor deposition (CVD) and physical vapor deposition (PVD), electrochemical method [16], chemical reduction process [17], sol-gel technique [18]. Thin films of it have also been deposited in vacuum by magnetron sputtering [19], thermal evaporation [20], molecular beam epitaxy [21], and laser pulsed deposition [22-23].

CO$_2$ lasers have been used to prepare films of ZnO, ZrO$_2$, graphite and organic film [24-27]. Choudhury et al. [28] prepared ZnSe films using a continuous wave CO$_2$ laser (CW-CO$_2$) onto substrates heated to 250°C. In this paper, a CW-CO$_2$ laser was used to deposit films by evaporation onto unheated glass substrates. This provides a lower cost technique of laser deposition. Films produced were then annealed to study the effect on structure and optical properties. Film structure, film thickness, surface morphology, and optical properties were analyzed by X-ray diffractometer (XRD), scanning electron microscope (SEM), atomic force microscope (AFM), and ultraviolet-visible spectroscopy (UV-vis), respectively.

Experimental

Materials

ZnSe thin films were prepared in a vacuum chamber by CW-CO$_2$ laser evaporation. The target was prepared by pressing pellets, 3.0 mm thick and 10 mm diameter, of 99.99% pure ZnSe powder (Balzers Coating Materials). The substrates are glass microscope slides (25 mm × 75 mm × 2 mm). The glass slides were cleaned in ethanol and acetone, and finally ultrasonically cleaned for 30 minutes in distilled water.

Method

The CW-CO$_2$ laser consisted of a sealed laser tube 40 cm long. The laser beam has a typical wavelength of 10.6 μm and a 3 mm diameter. The laser power output was fixed at 10 W for all samples. The laser beam was focused onto the target surface by a plano-convex lens with a 10 cm focal length. The distance between the focus lens and the ZnSe target was adjusted until a 1.0 mm spot size on the target surface was achieved. The working pressure in the vacuum chamber was fixed at 3×10^{-3} mbar. The CW-CO$_2$ laser evaporating process had a 30 min evaporation time and the substrate was at ambient temperature. **Fig. 1** shows the CW-CO$_2$ laser evaporation system diagram.
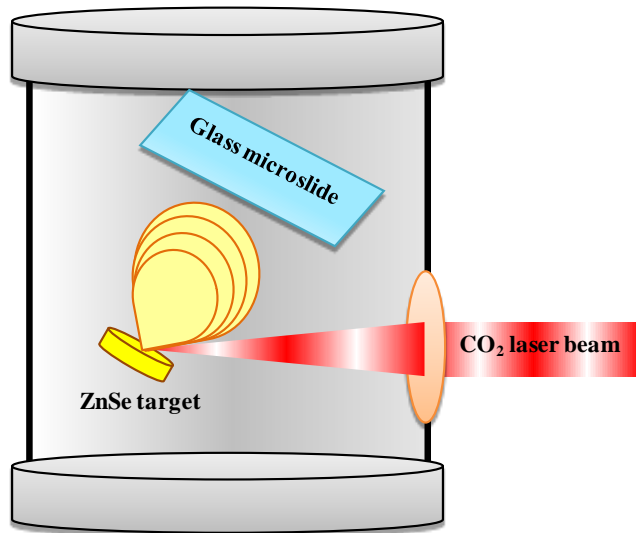

Fig. 1. Schmatic diagram of laser evaporation chamber with CW-CO$_2$ laser source.

Annealing was carried out at 100°C, 200°C and 300°C for one hour in an insulated box atop a hot plate (20 cm. diameter), temperature being measured and controlled by thermocouple. All samples had their crystal structure, surface morphology and RMS roughness, film thickness and optical properties determined by using XRD (Bruker D8 ADVANCE), AFM (SII Nanotechnology model SPA400), a LEO 1455VP SEM, and UV-vis (Jenway model 6715), respectively. The XRD radiation was CuKα of 0.154 nm wavelength. Scanning was performed from 20 to 60 2θ degrees at a scan rate of 0.2°/min. The UV-vis scan was between wavelengths of 400 nm and 900 nm.

Results and discussion

Fig. 2 shows the XRD patterns of the ZnSe thin films produced. The ZnSe thin film patterns of the as-deposited and 100°C, 200°C and 300°C annealed specimens showed a strong (111) peak of cubic ZnSe (zincblende).
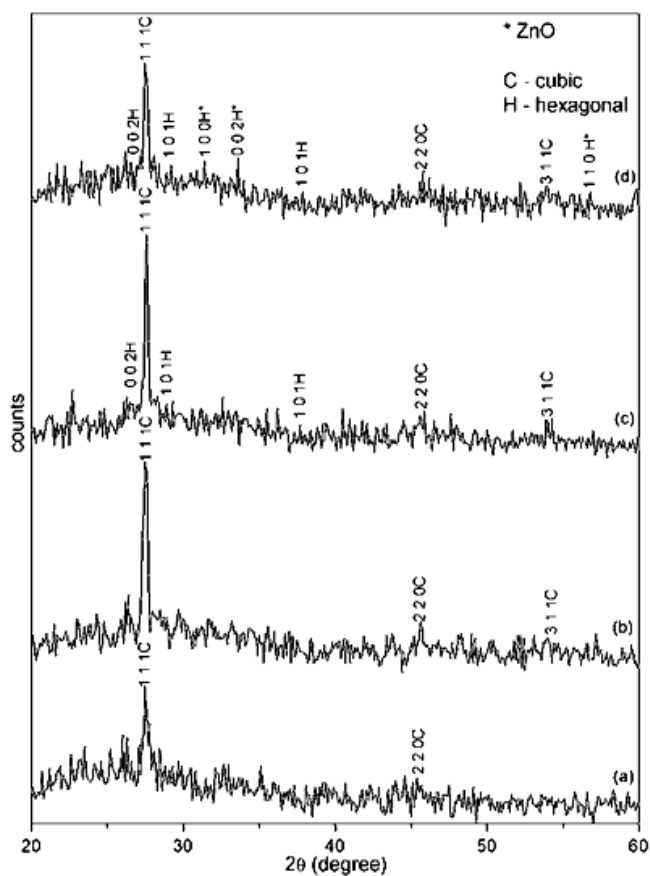
Fig. 2. XRD pattern of ZnSe thin films (a) as-deposited, annealed at **(b)** 100°C, **(c)** 200°C and **(d)** 300°C.

Fig. 2(a) displays the XRD pattern of the as-deposited ZnSe thin film, which shows the reflection peak (111), and (220). Annealing at 100°C adds a new zincblende reflection peak (311) (**Fig. 2(b)**). Thus, the as-deposited and 100°C annealed condition of the ZnSe thin films are the cubic phase of ZnSe (zincblende-type). On annealing at 200°C the hexagonal phase of ZnSe begins to develop (**Fig. 2(c)**). This phase transformation of ZnSe films with air annealing has been reported by Kale and Lokhande [29].

The XRD pattern of the ZnSe film annealed at 300°C shows new peaks that correspond to a ZnO phase, formed by oxidation as per the reaction [30]:

$$ZnSe + \frac{3}{2}O_2 \rightarrow ZnO + SeO_2 \qquad (1)$$
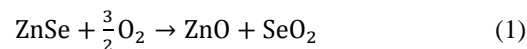
The XRD results show an increase in the intensity of the (111) peak for the ZnSe cubic structure with an increase in the annealing temperature from 100°C and 200°C, while the ZnSe film annealed at 300°C shows a decrease in the intensity of the (111) peak with a corresponding increase in ZnO formation. Khan et al. found that on annealing at

higher temperatures (about 400°C), the structure of ZnSe films changed from crystalline to amorphous [23].

The results from XRD patterns were used to calculate the average crystallite size (τ), the lattice spacing (d), the lattice parameter (a), the dislocation density (δ), and the strain (ε). The average crystallite size calculated from the Scherrer formula with show in equation (2) [23]

$$\tau = \frac{0.94\lambda}{\beta \cos \theta} \qquad (2)$$

where β is the full-width at half maximum (FWHM), λ is the wavelength of the X-ray radiation, and θ is the half angle between incident and the scattered X-ray.

The Bragg's formula was used to calculate the lattice spacing [23]

$$d = \frac{\lambda}{2 \sin \theta} \qquad (3)$$

The lattice parameter was determined by using this relation [23]:

$$\frac{1}{d^2} = \frac{h^2 + k^2 + l^2}{a^2} \qquad (4)$$

where h, k, and l represent the lattice planes

The dislocation density determined by using the relation [23]:

$$\delta = \frac{15\beta \cos \theta}{4a\tau} \qquad (5)$$

The film strain was determined by the following relation [23]:

$$\varepsilon = \frac{\beta \cos \theta}{4} \qquad (6)$$

Table 1 shows the values of the structural properties of the ZnSe thin films. The crystallite size of the as-deposited and the 100°C, 200°C and 300°C annealed films have values 23.84 nm, 34.70 nm, 49.64 nm and 34.42 nm, respectively estimated from the (111) reflection of cubic ZnSe. Crystallite size increased with an increase in annealing temperature up to 200°C. This increase in average crystallite size could be related to the existence of interface defects in the grain or crystallite boundaries induced by annealing. The values of strain and the dislocation density were found to decrease with the increase of annealing temperature from room temperature to 200°C as might be expected. At 300°C, the average crystallite size decreases, probably the result of the oxidation phase transformation and/or the fact that the size was calculated from only the (111) plane of cubic ZnSe. The values of strain and the dislocation density increase again, which may be related to crystallite size and also the development of the ZnO phase.

The surface morphology of the ZnSe thin film were observed by AFM. The results from AFM images showed

the film surface of as-deposited (**Fig. 3a**) and the 300°C annealed (**Fig. 3b**) which were indicated that the films are smooth, continuous and without cracks or pinholes. The photographs also revealed that the average crystallite size increases with the annealing temperature, which confirms the XRD results (**Table. 1**).
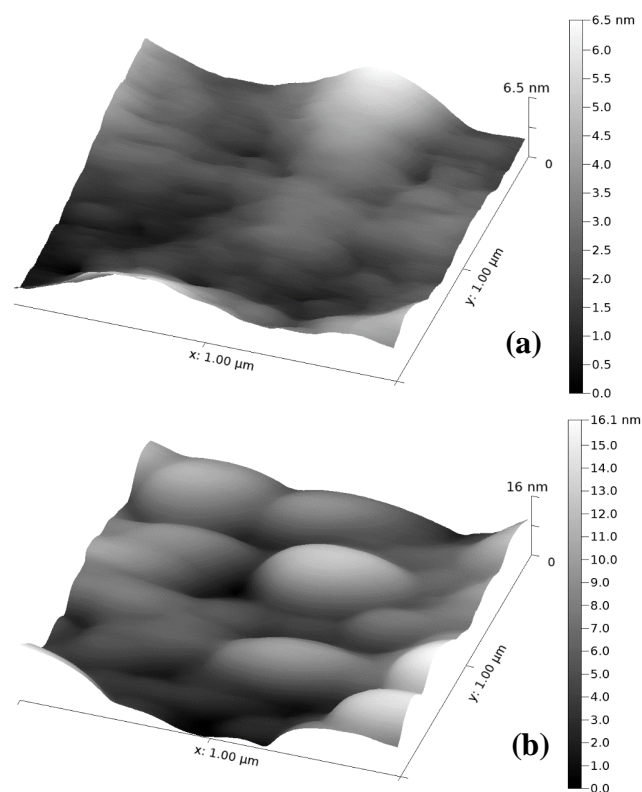
Fig. 3. Three dimensional AFM of ZnSe films; (a) as-deposited and (b) 300°C annealed.
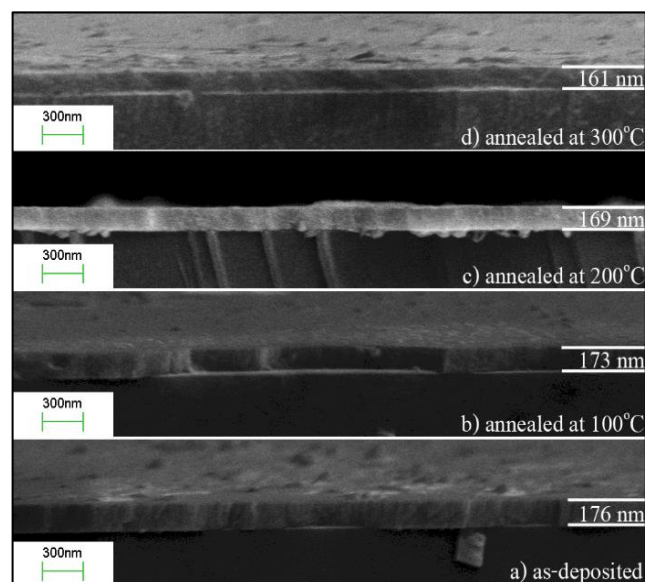
Fig. 4. SEM Image of ZnSe thin films (a) as-deposited, annealed at (b) 100°C, (c) 200°C and (d) 300°C.

The RMS roughness of the film increases when the annealing temperature increased. The RMS roughness of

Table 1. The structural parameters and properties of cubic ZnSe films at various annealing temperature.

Sample	2θ(deg.)	$h\,k\,l$	β(deg.)	a(Å)	d(Å)	τ(nm)	$\varepsilon \times 10^{-3}$ (lin^{-2}m^{-4})	$\delta \times 10^{15}$ (lin m^{-2})
As-deposited	27.50	1 1 1	0.358	5.609	3.238	23.84	1.518	1.703
	45.39	2 2 0						
	–	–						
Annealed at 100 °C	27.50	1 1 1	0.246	5.609	3.238	34.70	1.043	0.804
	45.66	2 2 0						
	53.98	3 1 1						
Annealed at 200 °C	27.59	1 1 1	0.172	5.590	3.228	49.64	0.729	0.394
	45.60	2 2 0						
	53.94	3 1 1						
Annealed at 300 °C	27.50	1 1 1	0.248	5.609	3.238	34.42	1.051	0.817
	45.80	2 2 0						
	53.95	3 1 1						

as-deposited film and 300°C annealed were 1.49 nm and 3.77 nm, respectively. In addition, the thickness of ZnSe thin film were decreased from 176 nm, 173 nm, 169 nm, and 161 nm when as-deposited and after annealing at 100°C, 200°C and 300°C, respectively. They were showed by SEM images (**Fig. 4**).

The transmission spectra of the ZnSe films were observed by UV-Vis at wavelengths between 400 nm to 900 nm. The ZnSe thin film transmission spectra of the as-deposited and annealed are clearly differentiated (**Fig. 5**).

The UV-Vis spectra were used to estimate the optical band-gap energy (E_g) of the ZnSe thin films by Eq. (7)

$$\alpha = \frac{A}{h\nu}\left(h\nu - E_g\right)^{1/2} \qquad (7)$$

where α is the absorption coefficient, $h\nu$ is the incident photon energy A is the characteristic parameter. The α was calculated by Eq. (8)

$$\alpha = \frac{1}{D}\ln\frac{(1-R)^2}{T} \qquad (8)$$

where D is the film thickness, R is the reflection coefficient and T is the transmission coefficient. The $(\alpha h\nu)^2 = f(h\nu)$ relation was used to estimate the E_g value by extrapolating the portions ($(\alpha h\nu)^2 = 0$).
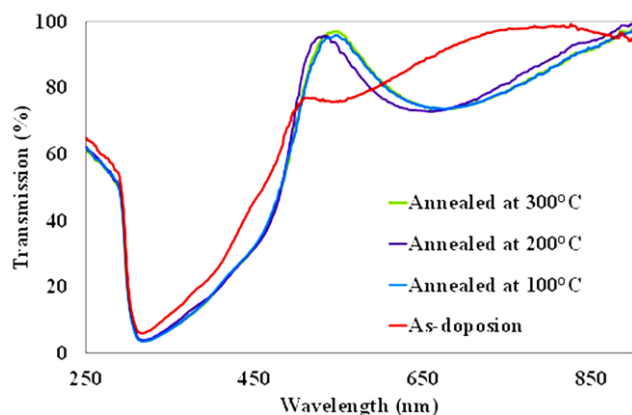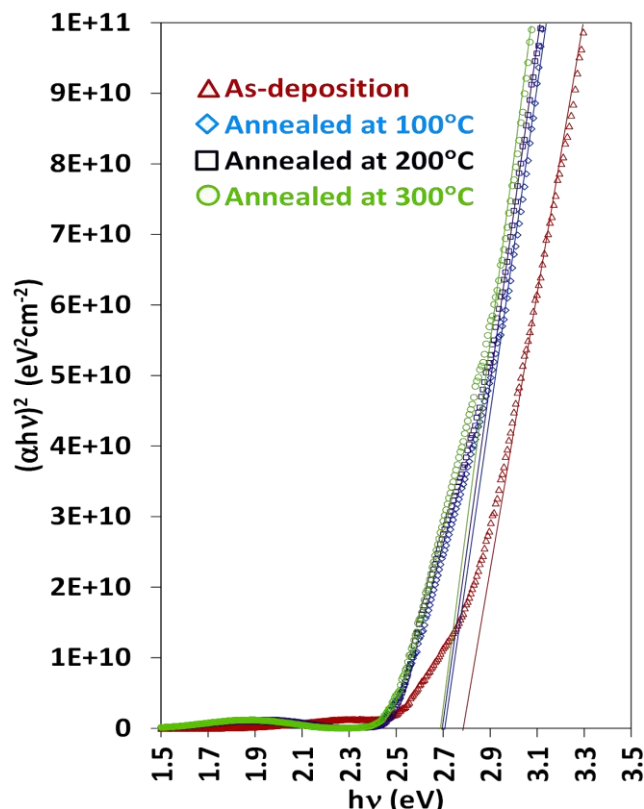
Fig. 6 shows the E_g estimation of the as-deposited and annealed ZnSe film. The E_g value of the as-deposited ZnSe film is 2.76 eV which shows a "blue-shift" of 0.06 eV from 2.70 eV of the bulk material. The band gap energy decreased with the air annealing. With the annealing process, the E_g value of ZnSe thin films decreased to 2.72 eV, 2.70 eV and 2.69 eV when the annealing temperature increased to 100°C, 200°C, and 300°C, respectively. This decreasing trend is explained by the average crystallite size increasing. This phenomenon has been explained by the quantum size effect in materials [23]. When the crystallite size increases and grain boundaries decrease minimizing the scattering and resulting with E_g increasing. At the 300°C annealing condition the crystallite size decreases and the E_g value decreased.

Fig. 5. Optical transmittance spectra of ZnSe thin films (a) as-deposited, annealed at (b) 100°C, (c) 200°C and (d) 300°C.

Fig. 6. Plot of $(\alpha h\nu)^2$ vs. $h\nu$ of ZnSe films; at as-deposited, annealed at 100 °C, 200 °C, and 300 °C.

Conclusion

This work has shown that CW-CO_2 laser deposition of ZnSe films onto cold substrates is a viable alternative to deposition onto heated substrates. In addition, annealing can be used to control structure, crystallite size and band gap energy. The ZnSe thin films were deposited onto glass substrates by CW-CO_2 laser evaporation and were annealed at 100°C to 300°C. AFM showed the films to be homogeneous. The structure of the as-deposited and 100°C annealed films were found to be cubic. At 200°C, the film structure began to transform to from a cubic to a hexagonal structure. At 300 °C, the film began to degrade to ZnO. The average crystallite size increased when the annealing temperature increased. The E_g value of the as-deposited film is 2.76 eV and the E_g values of annealed film are about 2.70 eV. Moreover, the E_g values decreased when annealing temperature increased. Finally, the transparency of the ZnSe films was found to be ~80% between the optical ranges of 1.55 - 2.37 eV; this is similar to the transparency found by Khan and Lokhande [29] recently. The lack of a pre-heated substrate and the ability to control band gap energy by annealing provides a versatile alternative source of ZnSe film deposition for potential optoelectronic applications.

Reference

1. Bourenane, K.; Keffous, A.; Nezzal G.; *Vacuum*, **2007**, *81*, 663-668.
   DOI: 10.1016/j.vacuum.2006.09.009
2. Lokeswara, G.V.; Reddy, Rama Moorthy, L.; Chengaiah, T.; Jamalaiah. B.C.; *Adv.Mat. Lett.*, **2013**, *4*: 841.
   DOI: 10.5185/amlett.2013. 3453
3. Szerling, A.; Karbownik, P.; Łaszcz, A.; Kosiel, K.; Bugajski, M.; *Vacuum*, **2008**, *82*, 977–981.
   DOI: 10.1016/j.vacuum.2008.01.006
4. Yamazoe, N.; Shimanoe, K.; *Sens. Actuat. B: Chemical*, **2013**, *187*, 162.
   DOI: 10.1016/j.snb.2012.10.048
5. Muthukumarasamy, N.; Velumani, S.; Balasundaraprabhu, R.; CJayakumar, R.; Kannan, M.D.; *Vacuum*, **2010**, *84*, 1216-1219.
   DOI: 10.1016/j.vacuum.2009.10.028
6. Phae-ngam, W.; Kosalathip, V.; Kumpeerapun, T.; Limsuwan, P.; Dauscher, A.; *J. Appl. Sci.*, **2011**, *11*, 3625.
   DOI: 10.3923/jas.2011.3625.3629
7. Soylu, M.; *Vacuum*, **2014**, *106*, 33.
   DOI: 10.1016/j.vacuum.2014.03.008
8. Wang, H.; Wu, Z.; Liu, Y.; Sheng, Z.; *J.Mol.Cat. A: Chemical*, **2008**, *287*, 176.
   DOI: 10.1016/j.molcata.2008.03.010
9. Zhang, S.; *Cer. Int.*, **2014**, *40*, 4553.
   DOI: 10.1016/j.ceramint.2013.08.131
10. Dashora, A.; Patel, N.; Kothari, D.C.; Ahuja, B.L.; Miotello, A.; *Solar Energ. Mat. Solar Cells*, **2014**, *125*, 120.
    DOI: 10.1016/j.solmat.2014.02.032
11. Cavalcante, L.S.; Batista, N.C.; Badapanda, T. ; Costa, M.G.S. ; Li, M.S.; Avansi, W.; Mastelaro, V.R.; Longo, E.; Espinosa, J.W.M.; Gurgel, M.F.C.; Zdanowicz, T.; Rodziewicz, T.; Zabkowska-Waclawek M.; *Mat.Sci. Semicond. Process.* 2013, 16, 1035.
    DOI: 10.1016/j.mssp.2012.12.010
12. Huang, C.W.; Weng, H.M.; Jiang, Y.L.; Ueng, H.Y.; *Vacuum*, **200**8, *83*, 313-319.
    DOI: 10.1016/j.vacuum.2008.06.004
13. Chen, L.; Lai, J.S.; Fu, X.N.; Sun, J.; Ying, Z.F.; Wu, J.D.; Lu, H.; Xu, N.; *Thin Solid Films*, **2013**, *529*, 76.
    DOI: 10.1016/j.tsf.2012.02.037
14. Xia, X.; Liu, Z.; Du, G.; Li, Y.; Ma, M.; Yao, K.; *J. Luminesce.* **2012**, 132, 100.
    DOI: 10.1016/j.jlumin.2011.07.025
15. Yablonskii, G.P.; Lutsenko, E.V.; Vainilovich, A.G.; Pavlovskii, V.N.; Ivanov, S.V.; Sedova, I.V.; Sorokin, S.V.; Kop'ev, P.S.; *J. Non-Cryst. Solids*, **2010**, 356, 1928.
    DOI: 10.1016/j.jnoncrysol.2010.05.038
16. Jia, L.; Kou, H.; Jiang, Y.; Yu, S.; Li, J.; Wang, C.; *Electrochim. Acta*, **2013**, *107*, 71–77.
    DOI: 10.1016/j.electacta.2013.06.004
17. Dhanasekaran,.; Mahalingam, T.; Rhee, J.K.; Chu, J.P.; *Optik,* **2013**, *124,* 255.
    DOI: 10.1016/j.ijleo.2011.11.063
18. Jiang, H.; Yao, X.; Che, J.; Wang, M.;, *Mat. Res. Bull.* **2006**, *41*, 2349–2356.
    DOI: 10.1016/j.materresbull.2006.04.013
19. Rizzo, A.; Tagliente, M.A.; Caneve, L.; Scaglione, S.; *Thin Solid Films*, **2000**, *368*, 8.
    DOI: 10.1016/S0040-6090(99)01104-9
20. Pardo Gonzalez, A.P.; Castro-Lora, H.G.; López-Carreño, L.D.; Martínez, H.M.; Torres Salcedo, N.J.; *J. Phys.Chem. Solids,* **2014**, *75*, 713.
    DOI: 10.1016/j.jpcs.2014.01.012
21. Tseng, Y.H.; Yang, C.S.; Wu, C.H.; Chiu, J.W.; Yang, M.D.; Wu, C.H.; *J. Cryst.Growth,* **2013**, *378*, 158.
    DOI: 10.1016/j.jcrysgro.2012.12.045
22. Boo, B.H.; Xu, N.; Lee, J.K.; *Vacuum*, **2002**, *64*, 145–151.
    DOI: 10.1016/S0042-207X(01)00384-0
23. Khan, T.M.; Zakria, M.; Ahmad, M.; Shakoor, R.I.; *J. Luminesce*, **2014**, *147*, 97.
    DOI: 10.1016/j.jlumin.2013.10.064
24. Yin, X.J.; Lai, G.R.; Chen, J.S.; Kao, J.S.; *Surf. Coat. Technol.*, **1997**, *90*, 239.
    DOI: 10.1016/S0257-8972(96)03150-7
25. Wei, C.; Deng, D.; Tian, G.; He, H.; Shao, J.; Fan, Z.; *Optik*, **2008**, *119*, 624–629.
    DOI: 10.1016/j.ijleo.2007.04.005
26. Kano, S.; Kohno, M.; Sakiyama, K.; Sasaki, S.; Aya, N.; Shimura, H.; *Chem.Phys. Lett.,* **2003**, *378*, 474.
    DOI: 10.1016/S0009-2614(03)01326-5
27. Grytsenko, K.; Lytvyn, O.; Ivanov, L.F.; Grakovich, P.N.; Sonntag, M.; Schrader, S.; *Appl. Surf. Sci.*, **2007**, *253*, 8028.
    DOI: 10.1016/j.apsusc.2007.02.080
28. Choudhury, M.G.M.; Islam, M.R.; Rahman, M.M.; Hakim, M.O.; Khan, M.K.R.; Kao, K.J.; Lai, G.R.; *Acta physica slovaca*, **2004**, 54, 417.
    ISSN: 1336-040X
29. Kale, R.B.; Lokhande, C.D.; *Appl. Surf. Sci.*, **2005**, *252*, 929.
    DOI: 10.1016/j.apsusc.2005.01.154
30. Chaparro, A.M.; Martínez, M.A.; Guillén, C.; Bayón, R.; Gutiérrez, M.T.; Herrero, J.; *Thin Solid Films*, **2000**, *361/362*: 177.
    DOI: 10.1016/S0040-6090(99)00791-9